JOURNAL OF MODERN OPTICS, 2000, VOL. 47, NO. 7, 1155–1169

# Switching and self-trapping dynamics of Bose–Einstein solitons

S. RAGHAVAN† and G. P. AGRAWAL‡

†Rochester Theory Center for Optical Science and Engineering, Department of Physics & Astronomy, University of Rochester, Rochester, NY 14627, USA

‡Rochester Theory Center for Optical Science and Engineering and The Institute of Optics, University of Rochester, Rochester, NY 14627, USA

(*Received 9 September 1999; revision received 9 November 1999*)

**Abstract.** We investigate the dynamics of two weakly coupled Bose condensates in long cigar-shaped traps. The Bose condensates are characterized by attractive mean-field interaction and consequently can be studied in terms of bright solitons. We exploit the analogy with directional fibre couplers in nonlinear fibre optics to uncover interesting dynamical regimes like switching of condensates from one trap to another and self-trapping of condensates. We also discuss the analogy between two weakly coupled Bose condensates and the Josephson junction in superfluids and superconductors.

## 1. Introduction

The phenomenon of Bose–Einstein condensation was observed a few years ago in a weakly interacting gas of laser-cooled alkali atoms confined to a magnetic trap [1]. Since this discovery, there has been an intensive theoretical and experimental study of diverse aspects of Bose–Einstein condensates (BECs). An important facet of the physics governing BECs is the issue of macroscopic phase coherence. The early demonstration that spatial phase coherence did indeed exist came through the observation of interference fringes in two overlapping condensates [2]. A related experiment measured the phase difference and its long-term stability between two condensates in different hyperfine spin states [3].

It has, therefore, been compelling to look upon a weakly-coupled system of two BECs as a Josephson junction linking two superfluids. Several issues have already been addressed theoretically in the limit of non-interacting atoms [4]. Dynamics involving small-amplitude Josephson oscillations [5, 6] has also been investigated. Semi-classical mean-field dynamics has been studied using the Gross–Pitaevskii equation (GPE) and interesting phenomena like macroscopic quantum self-trapping [7–9] and the existence of $\pi$-states (dynamical states wherein the time-averaged quantum phase difference across the junction equals $\pi$) [8, 9] have been predicted in weakly coupled double BECs forming a boson Josephson junction. Similar studies have been conducted to investigate driven two-component BECs [10]. Finite-temperature effects describing damping have also been studied [6, 11]. Quantum corrections have been studied to describe collapse and

*Journal of Modern Optics* ISSN 0950–0340 print/ISSN 1362–3044 online 
http://www.tandf.co.uk/journals

revival sequences [7, 12], different dynamical transitions and $\pi$-states [13], phase decoherence [14], phase squeezing [15], and phase diffusion and renormalization of oscillation frequencies [12].

The GPE describing the semiclassical BEC dynamics is a nonlinear Schrödinger equation which appears in many fields (such as nonlinear fibre optics, plasma physics and condensed matter physics) and can be solved exactly in some circumstances by using the inverse scattering method [16, 17]. It is well known that the GPE support solitonic solutions [17–25]. Bright solitons have been shown to exist in coherent atomic waves [18, 19] and in condensates with attractive inter-atom interaction [20, 21]. In the case of condensates with repulsive interaction, there has been work considering dark solitons [22–25] and bright gap solitons [25]. The closest analogy to a weakly coupled double BEC in nonlinear fibre optics [26] is provided by a directional fibre coupler [27, 28]. The energy transfer in such a device is governed by two coupled nonlinear Schrödinger equations and involves switching of solitons from one fibre core to another. It is thus useful to transfer some of the techniques and insights from this field to the field of BEC dynamics. Specifically, we consider in this paper the problem of switching dynamics of BEC solitons between two adjacent long asymmetric cigar-shaped traps.

## 2. Coupled Gross Pitaevskii equations

The basic equation governing the dynamics of a single BEC in a confining potential is given by the GPE,

$$i\hbar\frac{\partial\Psi(\mathbf{r},t)}{\partial t} = -\frac{\hbar^2}{2m}\nabla^2\Psi(\mathbf{r},t) + V(\mathbf{r})\Psi(\mathbf{r},t) + g_0|\Psi(\mathbf{r},t)|^2\Psi(\mathbf{r},t), \tag{1}$$

where $\Psi(\mathbf{r},t)$ is the condensate wavefunction and $g_0 = 4\pi\hbar^2 a/m$ is the interatom interaction strength characterized by the s-wave scattering length $a$. $V(\mathbf{r})$ is the confining potential given, in the case of harmonic traps, by

$$V(\mathbf{r}) = \tfrac{1}{2}m\omega_0^2(\rho^2 + \nu_z^2 z^2), \tag{2}$$

where $\rho^2 = x^2 + y^2$ and it has been assumed, as is the case for many current experimental situations, that the trap is cylindrically symmetric with the harmonic frequency in the radial direction, i.e. $\omega_0$. If we assume further that the trap geometry is cigar-shaped, we can take $\nu_z \ll 1$. Since a BEC bright soliton is formed only in the case of attractive interaction $(g_0 < 0)$, we focus on this case in this paper. For completeness, the case of repulsive interaction $(g_0 > 0)$ is discussed later. We note here, however, that because the sign of the inter-atomic interaction can be changed by the use of external magnetic fields, as shown by the experiments of the MIT group [29], our analysis has fairly wide applicability. Further, some of the considerations of [25] resulting in bright gap solitons from repulsive condensates may apply here. We introduce normalized variables such that

$$t' = \omega_0 t, \quad \rho' = \rho/a_0, \quad z' = z/a_0, \tag{3}$$

where $a_0 = (\hbar/m\omega_0)^{1/2}$ is the characteristic trap length in the radial direction. We further define $U = 2\pi a/a_0$ and rescale the wavefunction as $\Psi'(\mathbf{r},t) = \Psi(\rho,z,t)(a_0^3)^{1/2}$. For simplicity of notation, we drop the primes on rescaled variables and rewrite equation (1) as

$$\mathrm{i}\frac{\partial \Psi}{\partial t} = [-\tfrac{1}{2}\nabla^2 + \tfrac{1}{2}(\rho^2 + \nu_z^2 z^2) - 2U|\Psi^2]\Psi. \tag{4}$$

We now consider two identical cigar-shaped traps separated from each other by a distance $d$. Following the work of Pérez-García *et al.* [21], we note that if the transverse confinement is much stronger than the confinement along the $z$ direction and the transverse shape of the wavefunction does not change much in each trap, we can write the solution of equation (4) as

$$\Psi(\rho, z, t) = R_1(\rho + d/2)\psi_1(z, t) + R_2(\rho - d/2)\psi_2(z, t), \tag{5}$$

where $\rho = 0$ occurs in the middle of the two traps. Noticing that $R_1(\rho)$ and $R_2(\rho)$ satisfy the eigenvalue problem of the two-dimensional isotropic harmonic oscillator, we can use the ground-state solution $R_0(\rho) \sim \exp(-\rho^2/2)$ for both of them. This procedure results in the following coupled one-dimensional equations:

$$\mathrm{i}\frac{\partial \psi_1}{\partial t} = -\frac{1}{2}\frac{\partial^2 \psi_1}{\partial z^2} - U|\psi_1|^2\psi_1 + \tfrac{1}{2}\nu_z^2 z^2\psi_1 + E_0\psi_1 + \mathcal{K}\psi_2, \tag{6}$$

$$\mathrm{i}\frac{\partial \psi_2}{\partial t} = -\frac{1}{2}\frac{\partial^2 \psi_2}{\partial z^2} - U\ \psi_2|^2\psi_2 + \tfrac{1}{2}\nu_z^2 z^2\psi_1 + E_0\psi_2 + \mathcal{K}\psi_1, \tag{7}$$

where $E_0$ is the ground-state energy and $\mathcal{K}$ is the linear coupling coefficient arising out of overlaps of the transverse parts of the wavefunctions. The $E_0$ term can be eliminated by using the transformation $\psi_j \to \psi_j \exp(-\mathrm{i}E_0 t)$ $(j = 1, 2)$.

If we assume, like in [21], that the confinement in the $z$ direction is weak compared to the condensate's self-interaction, the condensate is stabilized in the longitudinal direction solely as a result of competition between the kinetic energy (dispersion) and the nonlinear attraction. By neglecting the trap term, the coupled BEC system can be described by the following two coupled nonlinear Schrödinger equations:

$$\mathrm{i}\frac{\partial \psi_1}{\partial t} = -\frac{1}{2}\frac{\partial^2 \psi_1}{\partial z^2} - U|\psi_1|^2\psi_1 + \mathcal{K}\psi_2, \tag{8}$$

$$\mathrm{i}\frac{\partial \psi_2}{\partial t} = -\frac{1}{2}\frac{\partial^2 \psi_2}{\partial z^2} - U|\psi_2|^2\psi_2 + \mathcal{K}\psi_1. \tag{9}$$

This set of equations is quite similar to the one encountered in the study of soliton dynamics of directional fibre couplers [26–28]. We follow here, in particular, the work of Kivshar [28]. In the absence of inter-trap coupling ($\mathcal{K} = 0$), the two traps behave independently with the well-known groundstate solution in the form of a bright soliton:

$$\psi_j(z, t) = \frac{N_j}{2}U^{1/2}\mathrm{sech}\left(\frac{N_j U z}{2}\right)\exp(\mathrm{i}\phi_j) \qquad (j = 1, 2), \tag{10}$$

where $N_j = \int |\psi_j(z, t)|^2 \mathrm{d}z$ is the number of atoms in trap $j$ and $\phi_j(t) = (N_j U/2)^2 t$. Since only phase of the wavefunction changes with time, $N_j$ is time-dependent and all atoms remain confined to the trap indefinitely. As we shall see below, this situation changes when the two traps are close enough that the tails of the wavefunctions begin to overlap and $\mathcal{K} \neq 0$. We use the standard Lagrangian formulation [28] to solve equations (8) and (9) approximately.

## 3. Lagrangian formulation

It is well known [28] that the coupled GPEs, (8) and (9), can be derived from the Lagrangian

$$L(t,z) = \sum_{j=1}^{2}\left(\frac{\mathrm{i}}{2}[\psi_j^*\dot{\psi}_j - \psi_j\dot{\psi}_j^*] - \frac{1}{2}\left|\frac{\partial\psi_j}{\partial z}\right|^2 + \frac{U}{2}|\psi_j|^4\right) - \mathcal{K}(\psi_1^*\psi_2 + \psi_1\psi_2^*). \tag{11}$$

Our strategy is to assume that in the presence of relatively weak coupling between the two traps, the wavefunctions $\psi_j(t)$ retain the 'sech' shape given by equation (10) but the parameters $N_j, \phi_j$ become functions of $z, t$. We assume further, that the spatial dependence is weak compared to the temporal dependence. We thus define the effective Lagrangian as

$$\mathcal{L}(t) = \int L(t,z)\mathrm{d}z = -[\dot{\phi}_1(t)N_1(t) + \dot{\phi}_2(t)N_2(t)]$$

$$+\frac{U^2}{24}[N_1(t)^3 + N_2(t)^3] - \frac{4\mathcal{K}}{N_\mathrm{T}}N_1(t)N_2(t)\mathcal{I}(p)\cos[\phi_1(t) - \phi_2(t)], \tag{12}$$

where $N_\mathrm{T} = N_1 + N_2$ is the total number atoms in both traps (a conserved quantity), $p(t) = (N_2(t) - N_1(t))/N_\mathrm{T}$ the normalized population difference between the two traps, and

$$\mathcal{I}(p) = \int_0^\infty \frac{\mathrm{d}z'}{\cosh^2 z' + \sinh^2(z'p)}. \tag{13}$$

The equations of motions for $N_1(t)$, $N_2(t)$, $\phi_1(t)$, and $\phi_2(t)$ are obtained from the effective Lagrangian using

$$\frac{\mathrm{d}}{\mathrm{d}t}\frac{\partial\mathcal{L}}{\partial\dot{N}_j} = \frac{\partial\mathcal{L}}{\partial N_j}, \qquad \frac{\mathrm{d}}{\mathrm{d}t}\frac{\partial\mathcal{L}}{\partial\dot{\phi}_j} = \frac{\partial\mathcal{L}}{\partial\phi_j} \quad (j = 1,2). \tag{14}$$

Introducing the sum and difference variables and noting that $N_\mathrm{T}$ is a constant of motion while the total phase $\phi_\mathrm{T} = \phi_1(t) + \phi_2(t)$ does not play a significant role in the trap dynamics, we obtain the following two important equations for the fractional population difference $p(t)$ and the phase difference $\phi(t) \equiv \phi_2(t) - \phi_1(t)$:

$$\frac{\mathrm{d}p}{\mathrm{d}t} = (1 - p^2)\mathcal{I}(p)\sin\phi, \tag{15}$$

$$\frac{\mathrm{d}\phi}{\mathrm{d}t} = -\Lambda p + \cos\phi\frac{\mathrm{d}}{\mathrm{d}p}[(1 - p^2)\mathcal{I}(p)], \tag{16}$$

where we have rescaled the time to $2\mathcal{K}t$, and introduced our main dynamical parameter using

$$\Lambda = (UN_\mathrm{T})^2/(16\mathcal{K}). \tag{17}$$

Physically this parameter represents the relative strength of nonlinear interatom interaction in each trap with respect to the linear inter-trap coupling resulting from the proximity of two traps.

Equations (14) are integrable, as pointed out by Kivshar [28]. In fact, they can be derived from the conserved Hamiltonian

$$H = \tfrac{1}{2}\Lambda p^2 - (1 - p^2)\mathcal{I}(p)\cos\phi. \tag{18}$$

Note that the equations of motion as well as the conserved Hamiltonian have appeared in the context of directional fibre couplers [28]. Further, these equations are remarkably similar to those appearing in the context of nonlinear generalizations of Josephson-junction dynamics [7–9, 11]. The key difference between the system studied here and that of [7–9, 11] lies in the different ansatz used for the wavefunctions. Since nonlinear self-interaction dominates over the confining potential in the case studied here, our trial wavefunction has a 'sech' form. On the other hand, the system considered in [7–9, 11] was one where the trapping potential played a key role and the trial wavefunction, and hence the $N$ and $\phi$ dependence, were different.

## 4. Stationary states

The set of equations (15) and (16) cannot be integrated analytically. The source of difficulty stems from $\mathcal{I}(p)$ whose functional dependence on $p$ is through an integral. We have evaluated this integral numerically and fitted a sixth-degree polynomial to it. Only even powers of $p$ occur in the polynomial since $\mathcal{I}(p)$ is an even function of $p$. Surprisingly, we have found that $\mathcal{I}(p)$ is well approximated (relative error $< 1\%$) by a parabola of the form $\mathcal{I}(p) \approx 1 - \alpha p^2$, where $\alpha = 0.21$, over the entire range $-1 < p < 1$. This feature allows us to replace $\mathcal{I}(p)$ by $1 - \alpha p^2$ and obtain the following simplified set of two equations:

$$\frac{\mathrm{d}p}{\mathrm{d}t} = (1 - p^2)(1 - \alpha p^2) \sin \phi \equiv F(p, \phi), \tag{19}$$

$$\frac{\mathrm{d}\phi}{\mathrm{d}t} = -\Lambda p - 2p \cos \phi[(1 + \alpha) - 2\alpha p^2] \equiv G(p, \phi). \tag{20}$$

The stationary states are obtained by setting the time derivatives in equations (19) and (20) to zero. We find three stationary solutions of the form

$$\phi_0 = 0, p_0 = 0, \tag{21}$$

$$\phi_0 = \pi, p_0^2 = \frac{1}{2\alpha}\left(1 + \alpha - \frac{\Lambda}{2}\right), \tag{22}$$

$$\phi_0 = \cos^{-1}\left[\frac{-\Lambda}{2(1 - \alpha)}\right], p_0^2 = 1. \tag{23}$$

We refer to the first two states as the in-phase and out-of-phase solutions depending on whether the phase difference $\phi = 0$ or $\pi$. If one were to prepare two identical in-phase condensates such that $\phi_0 = 0$ and $p_0 = 0$, there will be no net population transfer and no dynamics provided the in-phase solution is dynamically stable. If the condensates are not identical in the sense that they have different atoms ($p_0 \neq 0$), the in-phase solution does not exist. Moreover, the out-of-phase stationary state exists only if $2(1 - \alpha) < \Lambda < 2(1 + \alpha)$, i.e. $\Lambda$ should lie between 1.58 and 2.42. The third solution clearly exists only for $2(\alpha - 1) < \Lambda < 2(1 - \alpha)$.

Before proceeding, we discuss the stability issue by performing a standard linear stability analysis for the stationary states. Introducing small fluctuations around the stationary solution, $p'(t) = p(t) - p_0$ and $\phi'(t) = \phi(t) - \phi_0$, and linearizing equations (19) and (20) in terms of them, we obtain a set of two linear equations

$$\frac{\mathrm{d}p'}{\mathrm{d}t} = F_p(p_0, \phi_0)p' + F_\phi(p_0, \phi_0)\phi', \tag{24}$$

$$\frac{\mathrm{d}\phi'}{\mathrm{d}t} = G_p(p_0, \phi_0)p' + G_\phi(p_0, \phi_0)\phi', \tag{25}$$

where a subscript denotes a derivative with respect to that variable. Assuming a solution of the form $p'(t) = \exp(gt)$, non-trivial solutions exist for values of $g$ given by

$$2g = (F_p + G_\phi) \pm [F_p - G_\phi)^2 + 4G_pF_\phi]^{1/2}. \tag{26}$$

We find that for all values of $p_0, \phi_0$, $F_p + G_\phi = 0$. Further, for the in-phase solution, we find $F_p = G_\phi = 0$, $F_\phi = 1$ and $G_p = -(\Lambda + 2 + 2\alpha)$. Since, $g$ is purely imaginary, and $\mathrm{Re}(g) = 0$ for all values of $\Lambda$, the in-phase solution is marginally stable. In the case of out-of-phase solution, we find

$$F_p = 0, \qquad F_\phi = -(1 - p_0^2)(1 - \alpha p_0^2), \tag{27}$$

$$G_p = -\Lambda + 2(1 + \alpha - 6\alpha p_0^2), \qquad G_\phi = 0. \tag{28}$$

The eigenvalue $g$ can then have a positive real part if $G_pF_\phi > 0$ or $\Lambda > 2(1 - \alpha)$. Since this solution exists only when $\Lambda > 2(1 - \alpha)$, we conclude that the out-of-phase solution is an unstable state and can be destroyed by small perturbations.

We now turn to the third solution. Here $F_p = -G_\phi = -2p_0(1 - \alpha)\sin\phi_0$, $F_\phi = 0$, and $G_p = -\Lambda - 2(1 - 5\alpha)\cos\phi_0$. The term under the square root in equation (26) thus becomes $16(1 - \alpha)^2 \sin^2\phi_0$ and consequently the eigenvalue $g$ can have a positive real part. Thus this solution is also unstable with respect to small perturbations.

## 5. Switching dynamics

Much of the dynamical behaviour of the system of equations (19) and (20) can be understood without actually having to write down the analytic solutions explicitly. Analytic solutions, however, can be obtained only in the limit of $\alpha = 0$ in equations (19) and (20) (see Appendix) and provide a qualitative understanding of the numerical results discussed below. We examine the dynamics of equations (19) and (20) for two initial conditions on the phase difference for which steady-state solutions exist: (a) $\phi(0) = \phi_0 = 0$ and (b) $\phi(0) = \phi_0 = \pi$. We plot in figure 1, changes in the fractional population difference $p(t)$ with time by using the initial conditions $p_0 = 0.6$, $\phi_0 = 0$. In figure 1 (*a*), the dotted and solid lines correspond to $\Lambda = 0$ and $\Lambda = 8$, respectively. In both cases, complete population transfer occurs between the two BECs in a periodic manner as $p$ oscillates between $-0.6$ and 0.6. However, the period and shape of oscillations depend on $\Lambda$. For $\Lambda = 0$ (strong inter-trap coupling case), oscillations are sinusoidal. As one increases the value of $\Lambda$, oscillations become highly non-sinusoidal.

A major qualitative change occurs when $\Lambda$ hits a critical value $\Lambda_c$. This case is shown in figure 1 (*b*) as a dashed line. Physically, the period of oscillations becomes infinite and $p(t)$ settles down to zero asymptotically. As $\Lambda$ is increased beyond this

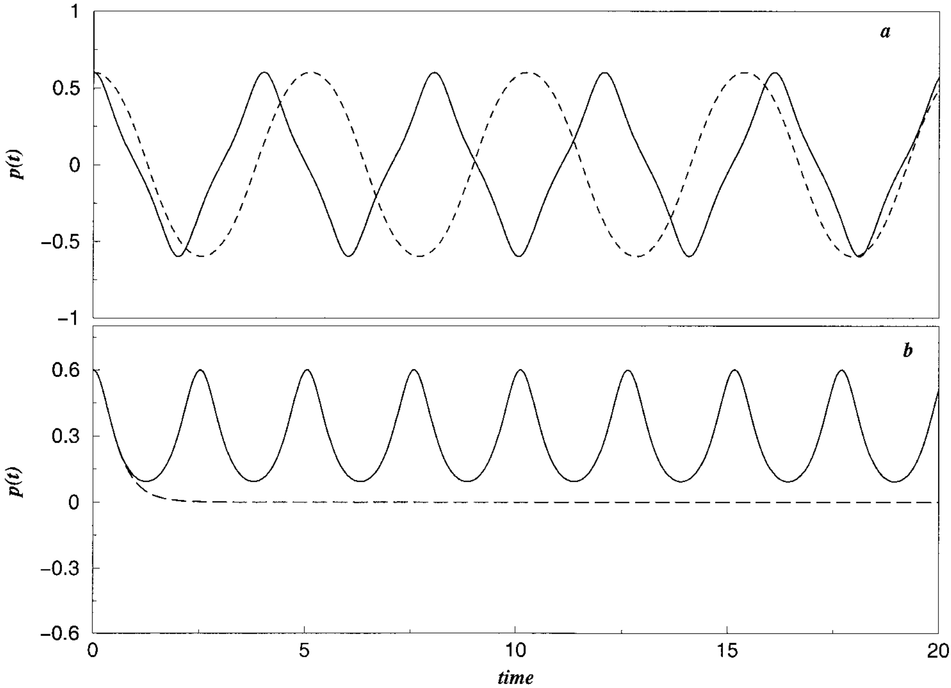


Figure 1. Population difference $p(t)$ against scaled dimensionless time with initial conditions $p_0 = 0.6$ and $\phi_0 = 0$; (*a*) $\Lambda = 0$ (dashed line), $\Lambda = 8$ (solid line); (*b*) $\Lambda = \Lambda_c = 8.8423$ (dashed line), $\Lambda = 9$ (solid line).

value, $p(t)$ begins to oscillate in a periodic manner once again with one major qualitative difference. As seen clearly in figure 1 (*b*), $p(t)$ oscillates asymmetrically and always remains positive, i.e. the time-averaged value of $p(t)(\equiv \langle p(t) \rangle)$ is non-zero. This feature implies 'macroscopic self-trapping' of the condensate with initially larger population. The BEC with initially larger population inhibits complete tunnelling when nonlinear coupling within that trap is much larger than the inter-trap coupling due to wavefunction overlap. This behaviour is very similar to the macroscopic quantum self-trapping discussed by Milburn *et al.* [7] and Smerzi and co-workers [8, 9] in the context of BECs and by Kenkre and co-workers in the context of polarons [30]. As explained in the next section, the threshold value $\Lambda_c$, can be calculated analytically as a function of the initial values $p_0$ and $\phi_0$.

We now discuss the out-of-phase initial condition, $\phi_0 = \pi$. Figure 2 shows the evolution of $p(t)$ with time using the same values of all other parameters. In particular, $p_0 = 0.6$ in all cases. The dotted line shows the $\Lambda = 0$ case (strong inter-trap coupling) in which the condensate populations execute complete sinusoidal oscillations. When $\Lambda$ is increased up to a critical value $\Lambda_s$, the system is placed in the out-of-phase stationary state discussed in section 4. No population transfer takes place when $p_0$ and $\Lambda_s$ satisfy the relation given in equation (22). Upon increase of $\Lambda$ beyond this value, the population in the denser condensate becomes self-trapped. Notice that this self-trapping differs from the in-phase case because now the condensate populations oscillate such that $\langle p(t) \rangle > p_0$: the initially more populated trap draws in condensate atoms from the lesser populated trap. This

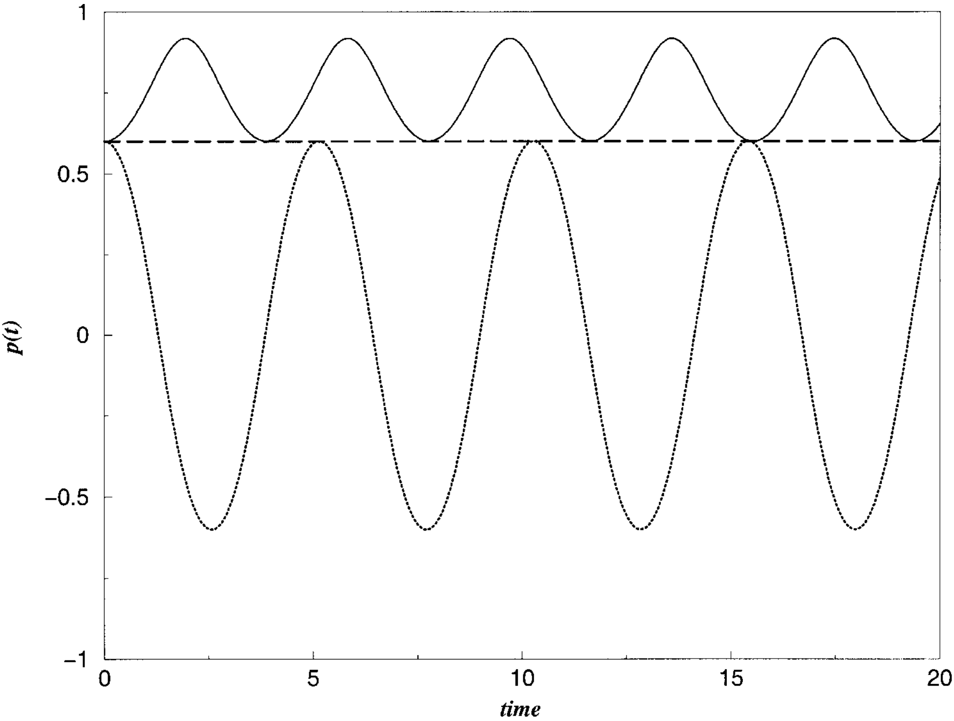


Figure 2. $p(t)$ versus scaled dimensionless time with the initial conditions $p_0 = 0.6$, $\phi_0 = \pi$ for $\Lambda = 0$ (dotted line), $\Lambda = \Lambda_s = 2.1167$ (dashed line), and $\Lambda = 3$ (solid line).

phenonemon is very similar to the amplitude transition discussed in the context of polarons by Tsironis and Kenkre [31] and in the context of BECs by Raghavan *et al.* [9].

We would like to point out here that $\Lambda$ could be changed most easily either (i) by changing the total number of atoms in the condensate, $N_T$, or (ii) by changing the spacing between the two traps (which controls the parameter $\mathcal{K}$). Furthermore, since $\Lambda$ is proportional to $N_T^2$, (17), the behaviour of the system would be more sensitive to change in $N_T$ than discussed in earlier studies of tunnelling and self-trapping in coupled BECs [7–9, 11], where the dependence between $\Lambda$ and $N_T$ was linear.

## 6. Potential-field analogy

As has been stressed in the contexts of soliton dynamics of fibre couplers by Paré and Florjańczyk [32], polaron dynamics in condensed matter physics by Kenkre and collaborators [33, 34], and tunnelling dynamics in BEC by Raghaven *et al.* [9], it is instructive to view the dynamical variable $p(t)$ as if it were a coordinate of a classical particle moving in a potential field. To do this, we start from the set of equations (19) and (20), eliminate the phase variable $\phi$ using the conserved Hamiltonian, and obtain the following equation of motion for $p(t)$ alone:

$$\frac{\mathrm{d}p}{\mathrm{d}t} = [V_0 - V(p)]^{1/2}, \tag{29}$$

where the $p$-potential is given by

$$V(p) = \frac{\Lambda^2}{4}p^4 - \Lambda H_0 p^2 - [(1-p^2)(1-\alpha p^2)]^2, \tag{30}$$

$$V_0 = V(p_0) + [(1-p_0^2)(1-\alpha p_0^2)\sin\phi_0]^2, \tag{31}$$

$$H_0 = \frac{\Lambda}{2}p_0^2 - (1-p_0^2)(1-\alpha p_0^2)(1-\alpha p_0^2)\cos\phi_0, \tag{32}$$

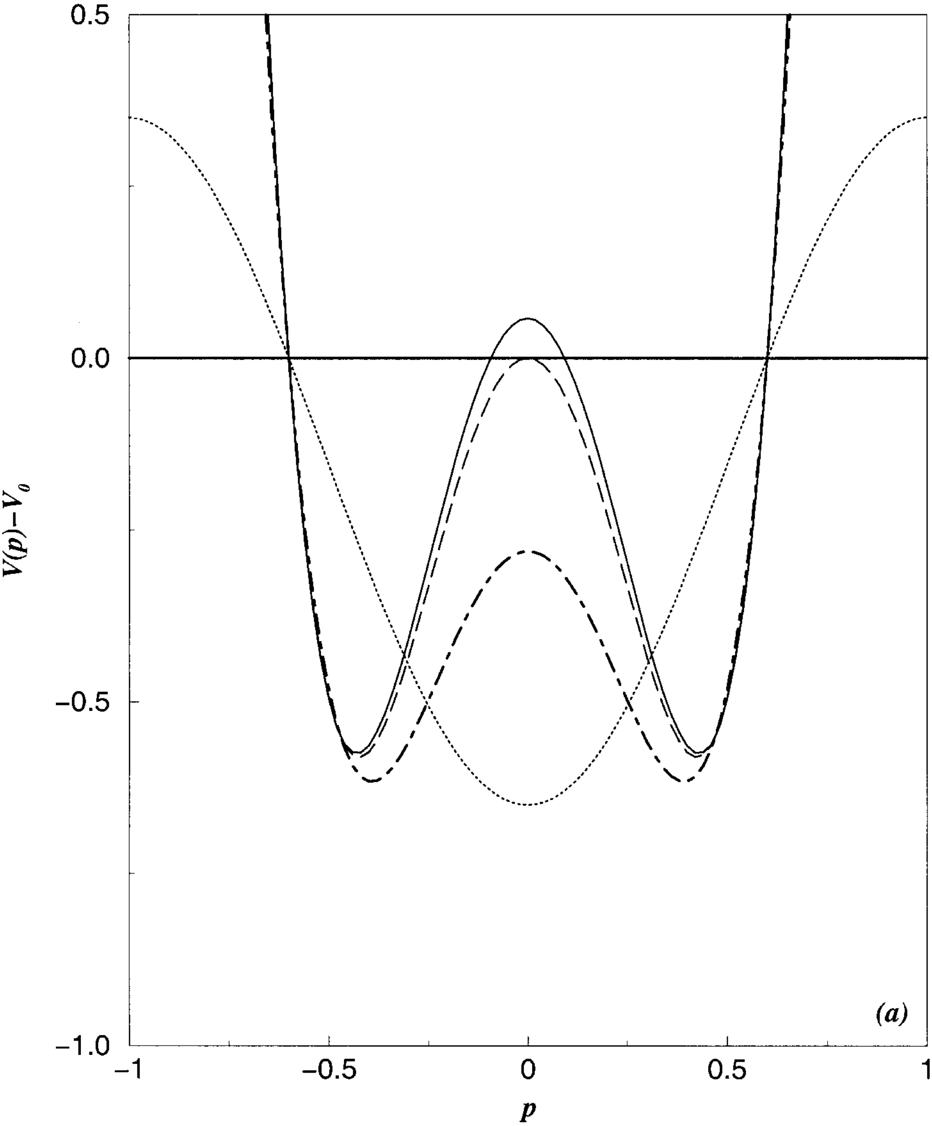


Figure 3 (*a*). Potential plots of $V(p) - V_0$ versus $p$. $p_0 = 0.6$, $\phi_0 = 0$ and $\Lambda$ takes on the values 0 (dotted line), 8 (dot-dashed line), $\Lambda_c = 8.8423$ (dashed line) and 9 (solid line).

where $V_0$ is a the total (conserved) energy computed at the initial values $p = p_0$, $\phi = \phi_0$. It is straightforward to plot the function $V(p) - V_0$ and look for allowed regions of oscillations in the $p$-space. Figure 3 ($a$) shows this for the parameter values used in figure 1. For $\Lambda = 0$ (dotted line), $V(p)$ has a single minimum located at $p = 0$ and $p$ oscillates about this average value in the range $-0.6 < p < 0.6$. For $\Lambda = 8$ (dot-dashed line), the potential changes qualitatively in such a way that $V(p)$ has two minima located symmetrically on each side of the value $p = 0$ where a local maximum occurs. However, since the peak located at $p = 0$ is below $V_0$, the $p$-particle has enough energy to cross over the peak. As a result complete oscillations

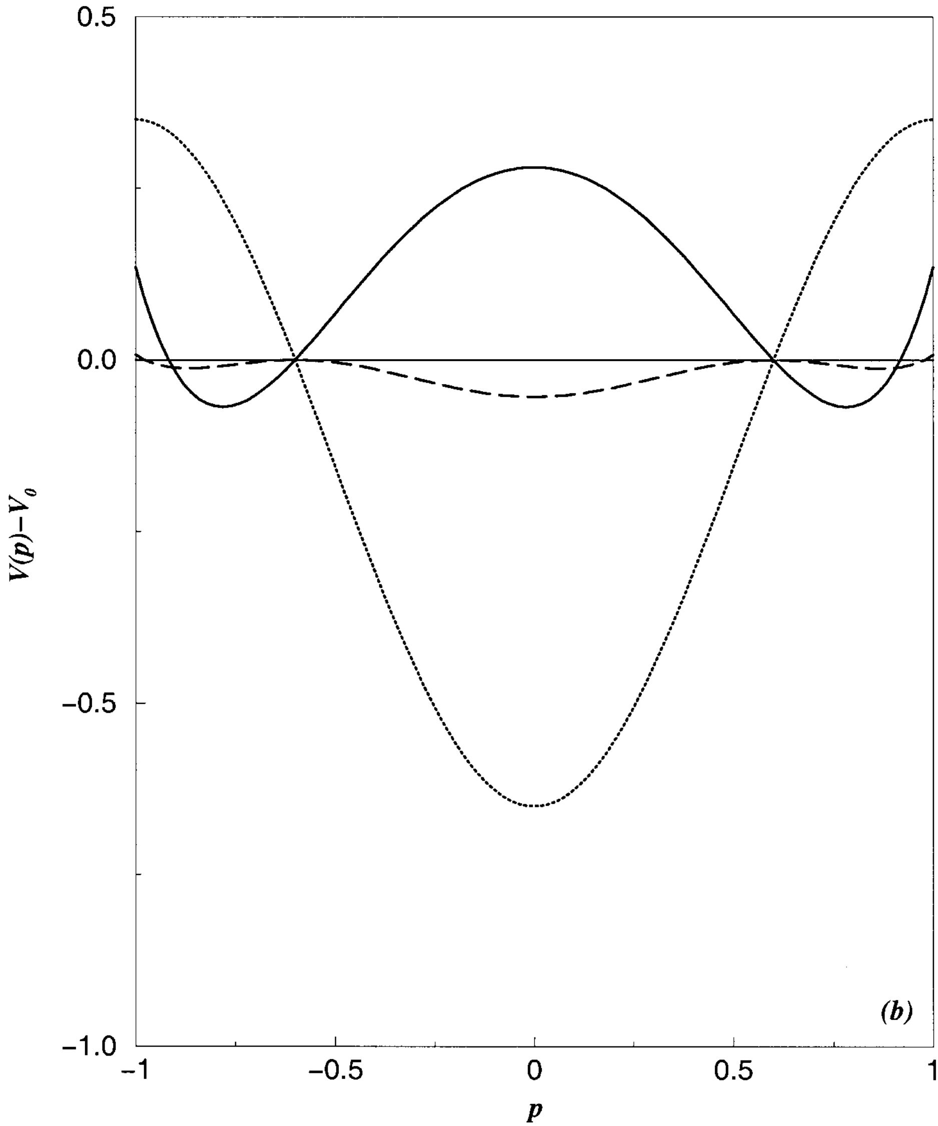


Figure 3 ($b$). Potential plots of $V(p) - V_0$ versus $p$. $p_0 = 0.6$, $\phi_0 = \pi$ and $\Lambda$ takes the values 0 (dotted line), $\Lambda_s = 2.1167$ (dashed line) and 3 (solid line).

in the range $-0.6 < p < 0.6$ can occur except that their shape will be highly non-sinusoidal because of the potential peak occurring at $p = 0$ for $\Lambda = 8$.

The situation changes qualitatively when the peak located at $p = 0$ becomes high enough that $V(p) > V_0$. Now the $p$-particle does not have enough energy to cross over the peak and is confined to the valley in which it is initially located. The transition occurs at $\Lambda = \Lambda_c$ (dashed line), and can be calculated from equations (30) by setting $V(p = 0) = V_0$ and is found to occur when

$$\Lambda_c = \frac{2}{p_0^2}[1 + (1 - p_0^2)(1 - \alpha p_0^2)\cos\phi_0], \tag{33}$$

provided $\cos\phi_0 > 0$. For the in-phase case shown in figure 1, $\Lambda_c = 8.63$ using $p_0 = 0.6$ and $\phi_0 = 0$. Beyond this value of $\Lambda$, as shown by the solid line of figure 3 (*a*), the $p$-particle is confined to the valley in which it is initially located, i.e. $\langle p(t)\rangle \neq 0$. This situation corresponds to self-trapping of the denser BEC.

We now investigate the out-of-phase case in which $\cos\phi_0 < 0$. We show in figure 3 (*b*), the potential plots for parameters used in figure 2 ($p_0 = 0.6$, $\phi_0 = \pi$) for values of $\Lambda$ in the range of 0 to 3. For $\Lambda = 0$ (dotted line), the potential is parabolic and the particle can oscillate freely. However, when $\Lambda = \Lambda_s$ (dashed line), the system is put into a stationary state. It is clear that since this point is a local maximum, this stationary state is unstable and any small perturbation will destroy this state. This is in contrast to the stationary states discussed by Tsironis and Kenkre [31] and Raghavan *et al.* [9] wherein all stationary states are stable. Further increase of $\Lambda$ (solid line) breaks the $p$-symmetry and the $p$-particle is self-trapped. Note also that the particle can only move towards increasing values of $p$ since the minimum of the $p$-potential occurs for $p > p_0$ as shown by the solid curve, i.e. $\langle p(t)\rangle > p_0$. Since the transition occcurs not when $V(p = 0) = V_0$ but the local maximum of $V(p)$ equal to $V_0$, the value of the transition, $\Lambda_s$ is different from $\Lambda_c$, and is given by

$$\Lambda_s = 2[(1 + \alpha) - 2\alpha p_0^2], \tag{34}$$

and is the same value given in equation (22). For the in-phase case shown in figure 2, $\Lambda_c \approx 2.12$ using $p_0 = 0.6$ and $\phi_0 = \pi$.

## 7. Phase-space description

To understand the self-trapping behaviour as well as the dynamics of the phase difference $\phi(t)$ as simply as possible, we show in figure 4 the trajectories in the phase space formed by the two conjugate variables $p$ and $\phi$. Each trajectory or contour is constructed with a fixed value of $\Lambda$, $p_0$, $\phi_0$ and thus for a constant energy. However, the energy varies from one contour to another. The light solid lines correspond to the initial condition $p_0 = 0.6$ and $\phi_0 = 0$ while $\Lambda$ takes on values 0, 8, $\Lambda_c = 8.8423$ and 9 (trajectories marked as a, b, c and d, respectively). The dark solid lines correspond to the initial condition $p_0 = 0.6$ and $\phi_0 = \pi$ while $\Lambda$ takes on values 0, 2 and 2.2 (trajectories marked as A, B and C, respectively. The light solid lines show that as long as $\Lambda < \Lambda_c$ (trajectories a and b), the average values of $p$ and $\phi$ are locked to zero. At the transition point, $\Lambda_c$ (trajectory c), a separatrix forms and beyond that (trajectory d), $\phi$ runs without bound while the average value of $p$ becomes non-zero. This marks the onset of self-trapping. Notice

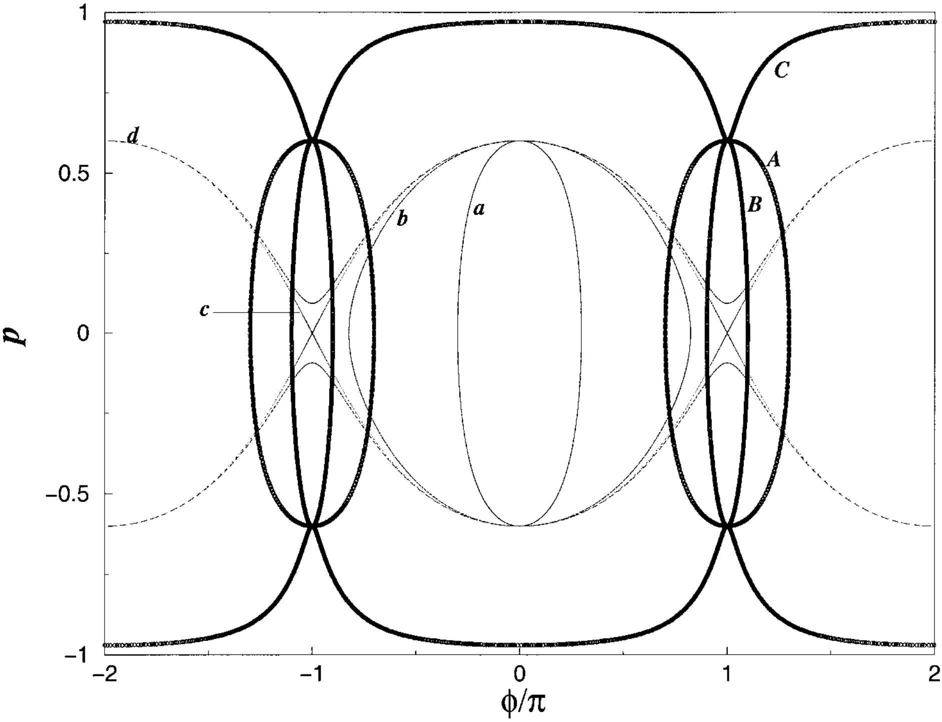


Figure 4. Phase-plane portrait formed by $p$ versus $\phi/\pi$. The light and dark solid lines correspond to in-phase ($\phi_0 = 0$) and out-of-phase coupling ($\phi_0 = \pi$) between the two condensates. In all cases $p_0 = 0.6$. For $\phi_0 = 0$, $\Lambda$ takes values: ($a$) 0, ($b$) 8, ($c$) $\Lambda_c = 8.8423$, and ($d$) 9. For $\phi_o = \pi$, $\Lambda$ takes the values: ($A$) 0, ($B$) 2, and ($C$) 3.

that increase of $\Lambda$ is always marked by an increase of the volume enclosed in the phase plane.

Now we come to the out-of-phase case and focus on the trajectories marked A, B and C. We see that as $\Lambda$ increases (curves A and B), the volume enclosed by the trajectory shrinks. At the transition point $\Lambda = \Lambda_s = 2.1167$, the trajectory becomes a point in phase space (not shown), indicating that formation of a stationary state (equation (22)). However, it is clear that this stationary state is unstable because any slight perturbation sends the system into drastically different trajectories. The trajectory C results when one increases $\Lambda$ beyond $\Lambda_s$. In this case, $\phi$ runs without beyond and $\langle p\rangle(t) \neq 0$ like the trajectory $d$. Note also that $\langle p\rangle(t) > p_0$ for trajectory C, and the population of the denser BEC can only increase.

## 8. Discussion and conclusion

We wish to add a few remarks here about switching dynamics of condensates with repulsive inter-atom interaction. We first note that in such a system the trap provides the confinement, and the condensate does not form a soliton. The condensate wave-function is, in fact, closer to that of a modified Gaussian as pointed out in earlier work [35]. Our preliminary investigations have shown that although the dynamics is extremely rich and perhaps possesses some chaotic aspects, the solutions are not solitonic in any sense.

To summarize, we have primarily discussed the switching and self-trapping dynamics of two BECs charcterized by attractive inter-atom interaction, in long cigar-shaped asymmetric traps that are weakly coupled in the radial direction. Because the BEC wavefunction takes the form of a bright soliton when the mean-field interaction among condensate atoms is attractive, the system is analogous in many respects to directional fibre couplers in nonlinear fibre optics. We make use of this analogy to study different aspects of the dynamical regimes and show that they are quite different from that found in earlier studies of tunnelling and self-trapping of Bose condensates. We have shown that among three possible steady states, only one is stable, when the two coupled BECs are identical in all respects. When the number of atoms in the two BECs are not the same, in general, population transfer will occur periodically. However, for a critical value of $\Lambda$, the nature of oscillations changes after a critical slowing down of the dynamics. This critical value of $\Lambda$ can be realized in experiments by changing either (i) the total number of atoms, $N_{\mathrm{T}}$, contained in both BECs or (ii) by adjusting the spacing between the two traps. Further, because of the quadratic dependence of $\Lambda$ on $N_{\mathrm{T}}$, the behaviour of the system could be very sensitive to change in $N_{\mathrm{T}}$.

**Acknowledgments**

We acknowledge the support of NSF Grant PHY94-15583.

**Appendix: Approximate analytic solutions**

One notes from equations (19) and (20) that because $\alpha = 0.21$, $\mathcal{I}(p) \approx 1$ for most values of $p$ in the range $-p_0 < p < p_0$ over which $p$ varies. The use of this approximation leads to the following simplified coupled equations for $p$ and $\phi$:

$$\frac{\mathrm{d}p}{\mathrm{d}t} = (1 - p^2)\sin\phi, \tag{A1}$$

$$\frac{\mathrm{d}\phi}{\mathrm{d}t} = -\Lambda p - 2p\cos\phi(t), \tag{A2}$$

with the conserved energy

$$H_0 = \frac{\Lambda p_0^2}{2} - (1 - p_0^2)\cos\phi_0. \tag{A3}$$

Equations (A1) and (A2) are simple enough that they be integrated analytically with a closed-form solution in terms of elliptic functions. The in-phase solution for $\phi_0 = o$ is given by:

$$p(t) = p_0 \,\mathrm{sn}\left[[(2+\Lambda)(4 - p_0^2(\Lambda+2))]^{1/2}(t - t_0)/2, p_0\left(\frac{(2-\Lambda)}{4 - p_0^2(\Lambda+2)}\right)^{1/2}\right], \Lambda < 2,$$

$$= p_0 \,\mathrm{cn}\left[[(\Lambda+2)(1 - p_0^2)]^{1/2} t, \frac{p_0}{2}\left(\frac{(\Lambda-2)}{(1-p_0^2)}\right)^{1/2}\right], 2 < \Lambda < \Lambda_{\mathrm{c}},$$

$$= p_0 \,\mathrm{dn}\left[\frac{p_0(1-p_0^2)}{2}\left(\frac{(\Lambda+2)}{(\Lambda-2)}\right)^{1/2} t, \frac{2}{p_0}\left(\frac{(1-p_0^2)}{(\Lambda-2)}\right)^{1/2}\right], \Lambda > \Lambda_c, \tag{A4}$$

where

$$t_0 = \frac{-2}{[(2+\Lambda)(4-p_0^2(\Lambda+2))]^{1/2}} F\left(\pi/2, p_0\left(\frac{(2-\Lambda)}{4-p_0^2(\Lambda+2)}\right)^{1/2}\right)$$

and $\Lambda_c = 2(2/p_0^2 - 1)$.

For $\phi_0 = \pi$ (out-of-phase case) the solution takes the form

$$p(t) = p_0 \,\mathrm{sn}\left[[(2-\Lambda)(4-p_0^2(2-\Lambda))]^{1/2}(t-t_0)/2, p_0\left(\frac{(2+\Lambda)}{4-p_0^2(2-\Lambda)}\right)^{1/2}\right], \Lambda < 2,$$

$$= \frac{p_0}{\mathrm{dn}\left[[(\Lambda-2)(4+p_0^2(\Lambda-2))]^{1/2} t/2, \left(\frac{4(1-p_0^2)}{(4+p_0^2(\Lambda-2))}\right)^{1/2}\right]}, \Lambda > 2. \tag{A5}$$

It is important to note that self-trapping always occurs when the $p$-particle potential energy $V(p)$ equals the total $p$-particle energy $V_0$ at $p = 0$. This translates to the condition that $H_0$ given by equation (A3) exceed unity. This happens when

$$\Lambda > \Lambda_c = \frac{2[1 + (1 - p(0)^2)\cos\phi(0)]}{p(0)^2}. \tag{A6}$$

For $\phi_0 = 0$, self-trapping occurs for $\Lambda_c = 2(2/p_0^2 - 1)$. For $\phi_0 = \pi$, however, equation (A6) implies that $\Lambda_c = 2$, independent of the initial population difference $p_0$.

## References


[1] Anderson, M. H., Matthews, M. R., Wieman, C. E., and Cornell, E. A., 1995, *Science*, **269**, 198; Davis, K. B., Mewes, M.-O., Andrews, M. R., van Druten, N. J., Durfee, D. S., Kurn, D. M., and Ketterle, W., 1995, *Phys. Rev. Lett.*, **75**, 3969; Bradley, C. C., Sackett, C. A., Tollett, J. J., and Hulet, R. G., 1995, *Phys. Rev. Lett.*, **75**, 1687; Fried, D. G., Killian, C., Willmann, L., Landhuis, D. L., Moss, S. C., Kleppner, D., and Greytak, T. J., 1998, *Phys. Rev. Lett.*, **81**, 3811; for a comprehensive bibliography of work in the field, see the Web page: http://amo.phy.gasou.edu/bec.html.

[2] Andrews, M. R., Townsend, C. G., Miesner, H.-J., Durfee, D. S., Kurn, D. M., and Ketterle, W., 1997, *Science*, **275**, 637.

[3] Hall, D. S., Matthews, M. R., Ensher, J. R., Wieman, C. E., and Cornell, E. A., 1998, **81**, 1539; 1998, *ibid.*, **81**, 1543.

[4] Javanainen, J., 1986, *Phys. Rev. Lett.*, **57**, 3164.

[5] Dalfovo, F., Pitaevskii, L., and Stringari, S., 1996, *Phys. Rev.* A, **54**, 4213.

[6] Zapata, I., Sols, F., and Leggett, A. J., 1998, *Phys. Rev.* A, **57**, R28.

[7] Milburn, C. J., Corney, J., Wright, E. M., and Walls, D. F., 1997, *Phys. Rev.* A, **55**, 4318.

[8] Smerzi, A., Fantoni, S., Giovannazzi, S., and Shenoy, S. R., 1997, *Phys. Rev. Lett.*, **79**, 4950.

[9] Raghavan, S., Smerzi, A., Fantoni, S., and Shenoy, S. R., 1999, *Phys. Rev.* A, **59**, 620.

[10] Williams, J., Walser, R., Cooper, J., Cornell, E., and Holland, M., 1999, *Phys. Rev.* A, **59**, R31; 1999, cond-mat/994399.

[11] Marino, I., Raghavan, S., Fantoni, S., Shenoy, S. R., and Smerzi, A., 1999, *Phys. Rev.* A, **60,** 487.
[12] Smerzi, A., and Raghavan, S., *Phys. Rev.* A (to appear).
[13] Raghavan, S., Smerzi, A., and Kenkre, V. M., 1999, *Phys. Rev.* A, **60,** R1787.
[14] Villain, P., Lewenstein, M., Dum, R., Castin, Y., You, L., Imamoglu, A., and Kennedy, T. A. B., 1997, *J. mod. Optics*, **44,** 1775.
[15] Steel, M. J., and Collett, M. J., 1998, *Phys. Rev.* A, **57,** 2920.
[16] Zakharov, V. E., and Shabat, A. B., 1973, *Sov. Phys.-JETP*, **37,** 823.
[17] Zakharov, V. E., and Shabat, A. B., 1972, *Sov. Phys.-JETP*, **34,** 62.
[18] Lenz., G., Meystre, P., and Wright, E. M., 1993, *Phys. Rev. Lett.*, **71,** 3271.
[19] Zhang, W., Walls, D. F., and Sanders, B. C., 1994, *Phys. Rev. Lett.*, **72,** 60.
[20] Ruprecht, P. A., Holland, M. J., Burnett, K., and Edwards, M., 1995, *Phys. Rev.* A, **51,** 4704.
[21] Pérez-García, V. M., Michinel, H., and Herrero, H., 1998, *Phys. Rev.* A, **57,** 3837.
[22] Reinhardt, W. P., and Clark, C. W., 1997, *J. Phys.* B, **30,** L785.
[23] Dum, R., Cirac, J. I., Lewenstein, M., and Zoller, P., 1998, *Phys. Rev. Lett.*, **80,** 2972.
[24] Hong, T., Wang, Y. Z., and Huo, Y. S., 1998, *Phys. Rev.* A, **58,** 3128.
[25] Zobay, O., Pötting, S., Meystre, P., and Wright, E. M., 1999, *Phys. Rev.* A, **59,** 643.
[26] Agrawal, G. P., 1995, *Nonlinear Fiber Optics*, 2nd edition (San Diego: Academic Press).
[27] Trillo, S., Wabnitz, S., Wright, E. M., and Stegeman, G. I., 1988, *Optics Lett.*, **13,** 672.
[28] Kivshar, Y. S., 1993, *Optics Lett.*, **18,** 7.
[29] Inouye, S., Andrews, M. R., Stenger, J., Miesner, H.-J., Stamper-Kurn, D.-M., and Ketterle, W., 1988, *Nature*, **392,** 151.
[30] Kenkre, V. M., and Campbell, D. K., 1986, *Phys. Rev.* B, **34,** 4949; Kenkre, V. M., 1989, *Singular Behavior and Nonlinear Dynamics*, edited by St. Pnevmatikos, T. Bountis and Sp. Pnevmatikos (Singapore: World Scientific).
[31] Tsironis, G. P., and Kenkre, V. M., 1998, *Phys. Lett.* A, **127,** 209.
[32] Paré, C., and Florjańczyk, M., 1990, *Phys. Rev.* A, **41,** 6287.
[33] Kenkre, V. M., and Kuś, M., 1992, *Phys. Rev.* B, **46,** 13792.
[34] Raghavan, S., Kenkre, V. M., and Bishop, A. R., 1997, *Phys. Lett.* A, **233,** 73.
[35] Pérez-García, V. M., Michinel, H., Cirac, J. I., Lewenstein, M, and Zoller, P., 1996, *Phys. Rev. Lett.*, **77,** 5320.